

ORIGINAL ARTICLE

OPEN

Hepatocyte-derived liver progenitor-like cells attenuate liver cirrhosis via induction of apoptosis in hepatic stellate cells

Xu Zhou^{1,2,3} | Wen-Ming Liu^{1,3,4} | Han-Yong Sun⁵ | Yuan Peng⁶ |
Ren-Jie Huang² | Cai-Yang Chen¹ | Hong-Dan Zhang² | Shen-Ao Zhou² |
Hong-Ping Wu⁷ | Dan Tang^{1,3} | Wei-Jian Huang¹ | Han Wu⁸ | Qi-Gen Li⁵ |
Bo Zhai⁶ | Qiang Xia⁵ | Wei-Feng Yu^{1,3} | He-Xin Yan^{1,2,3,6,9}

¹Department of Anesthesiology, Renji Hospital, Shanghai Jiaotong University School of Medicine, Shanghai, China

²Shanghai Celliver Biotechnology Co. Ltd., Shanghai, China

³Key Laboratory of Anesthesiology (Shanghai Jiao Tong University), Ministry of Education, Shanghai, China

⁴Institute for Regenerative Medicine, Shanghai East Hospital, School of Life Sciences and Technology, Tongji University, Shanghai, China

⁵Department of Hepatic Surgery, Renji Hospital, Shanghai Jiaotong University School of Medicine, Shanghai, China

⁶Department of Interventional Oncology, Renji Hospital, Shanghai Jiaotong University School of Medicine, Shanghai, China

⁷Molecular Epidemiology Laboratory, Eastern Hepatobiliary Surgery Hospital, Second Military Medical University, Shanghai, China

⁸Hubei Key Laboratory of Tumour Biological Behaviors, Department of Radiation and Medical Oncology, Zhongnan Hospital of Wuhan University, Wuhan, China

⁹Shanghai Cancer Institute, Renji Hospital, Shanghai Jiaotong University School of Medicine, Shanghai, China

Correspondence

He-Xin Yan, Department of Anesthesiology, Renji Hospital, Shanghai Jiaotong University School of Medicine, 160 Pujian Road, Pudong New District, Shanghai 200127, China.
Email: hexinyw@163.com.

Wei-Feng Yu, Department of Anesthesiology, Renji Hospital, Shanghai Jiaotong University School of Medicine, 160 Pujian Road, Pudong New District, Shanghai 200127, China.
Email: ywf808@yeah.net.

Qiang Xia, Department of Hepatic Surgery, Renji Hospital, Shanghai Jiaotong University School of Medicine, 160 Pujian Road, Pudong New District, Shanghai 200127, China.
Email: xiaqiang@shsmu.edu.cn.

Bo Zhai, Department of Interventional Oncology, Renji Hospital, Shanghai Jiaotong University School of Medicine, 160 Pujian Road, Pudong New District, Shanghai 200127, China.
Email: zhaiboshi@sina.com.

Abstract

Background: Cell therapy demonstrates promising potential as a substitute therapeutic approach for liver cirrhosis. We have developed a strategy to effectively expand murine and human hepatocyte-derived liver progenitor-like cells (HepLPCs) in vitro. The primary objective of the present study was to apply HepLPCs to the treatment of liver cirrhosis and to elucidate the underlying mechanisms responsible for their therapeutic efficacy.

Methods: The effects of allogeneic or xenogeneic HepLPC transplantation were investigated in rat model of liver cirrhosis. Liver tissues were collected and subjected to immunostaining to assess changes in histology. In vitro experiments used HSCs to explore the antifibrotic properties of HepLPC-secretomes and their underlying molecular mechanisms. Additionally, proteomic analysis was conducted to characterize the protein composition of HepLPC-secretomes.

Results: Transplantation of HepLPCs resulted in decreased active fibrogenesis and net fibrosis in cirrhosis models. Apoptosis of HSCs was observed

Abbreviations: AREG, amphiregulin; ECM, extracellular matrix; EGFR, epidermal growth factor receptor; HepLPCs, hepatocyte-derived liver progenitor-like cells; scrtms, secretomes; JAK, janus kinase; PHHs, primary hepatocytes; STAT, signal transducer and activator of transcription; TAA, thioacetamide.

Xu Zhou, Wen-Ming Liu, Han-Yong Sun, and Yuan Peng contributed equally to this work.

Supplemental Digital Content is available for this article. Direct URL citations are provided in the HTML and PDF versions of this article on the journal's website, www.hepcommjournal.com.

This is an open access article distributed under the terms of the Creative Commons Attribution-Non Commercial-No Derivatives License 4.0 (CCBY-NC-ND), where it is permissible to download and share the work provided it is properly cited. The work cannot be changed in any way or used commercially without permission from the journal.

Copyright © 2025 The Author(s). Published by Wolters Kluwer Health, Inc. on behalf of the American Association for the Study of Liver Diseases.

in vivo after HepLPC treatment. HepLPC-secretomes exhibited potent inhibition of TGF- β 1-induced HSC activation and promoted apoptosis through signal transducer and activator of transcription (STAT)1-mediated pathways in vitro. Furthermore, synergistic effects between amphiregulin and FGF19 within HepLPC-secretomes were identified, contributing to HSC apoptosis and exerting antifibrotic effects via activation of the janus kinase-STAT1 pathway.

Conclusions: HepLPCs have the potential to ameliorate liver cirrhosis by inducing STAT1-dependent apoptosis in HSCs. Amphiregulin and FGF19 are key factors responsible for STAT1 activation, representing promising novel therapeutic targets for the treatment of liver cirrhosis.

Keywords: AREG, FGF19, liver cirrhosis, liver progenitor cells

INTRODUCTION

Liver cirrhosis represents an advanced stage of hepatic fibrosis and constitutes a significant global burden in terms of morbidity and mortality.^[1] Approximately 1 million individuals die from liver cirrhosis annually, making it the 11th leading cause of death and, together with liver cancer, accounting for 3.5% of global fatalities.^[2] Clinically, decompensated liver cirrhosis is regarded as a terminal condition, with mortality being inevitable without liver transplantation. However, the scarcity of donor organs, coupled with surgical contraindications and complications, restricts transplantation to < 10% of eligible patients.^[3] Thus, mitigating disease progression and reducing liver transplantation rates emerge as primary clinical objectives in the management of liver cirrhosis, necessitating the implementation of innovative medical interventions.

Cell therapy for treating end-stage liver disease has rapidly developed, involving various cell types to remodel or replace damaged organs or tissues.^[4] There are mainly 3 types of cells used in the clinical treatment of liver diseases: adult primary hepatocytes (PHHs), fetal liver cells, and stem cells. PHHs are considered an ideal source for treating liver cirrhosis or failure and have been applied clinically. Hepatocyte transplantation aims to provide functional parenchymal support to the damaged liver, facilitating its recovery.^[5] However, transplanting 3%–5% of liver mass results in only 0.5% engraftment of the host liver.^[6] Due to the limited and difficult-to-expand sources of PHHs in vitro, alternative cell sources are being explored. Human fetal livers contain 2 stem cell niches: the ductal plates/canals of Hering, which harbor hepatic stem/progenitor cells,^[7] and peribiliary glands, which house biliary tree stem/progenitor cells.^[8] Both have been used in clinical trials to treat decompensated liver cirrhosis, showing improvements in multiple diagnostic and biochemical parameters with long-term effects.^[9] Compared to

PHHs, fetal liver stem/progenitor cells prove to be an ideal source due to their easier acquisition and cultivability. However, ethical concerns and the complex process of cell isolation and selection, which lacks standardization globally, contribute to the limited number of fetal liver cell therapy cases worldwide.^[10] Stem cells, including mesenchymal stem cells derived from bone marrow, umbilical cord, adipose tissue, teeth, and menstrual blood, as well as hematopoietic stem cells, bone marrow mononuclear cells, and endothelial progenitor cells, are used in clinical trials for managing liver fibrosis and cirrhosis.^[4] The required dose of stem cells is generally lower than that of hepatocytes, reflecting their primary mechanism of action through promoting the endogenous liver microenvironment via secreted bioactive molecules rather than direct replacement therapy. However, clinical results show the controversial therapeutic efficacy of stem cells for treating cirrhosis, possibly due to significant source variations, lack of standardized in vitro preparation processes, and heterogeneity between cell batches, leading to ambiguity in their clinical application.^[11] Overall, cells that have the ability to proliferate in vitro, like stem cells, and possess secretory function characteristics while also being derived from the liver may be the most promising option for cell therapy in liver disease.

We previously used a molecule combination strategy to generate novel hepatocyte-derived liver progenitor-like cells (HepLPCs) from primary hepatocytes.^[12,13] Through the analysis of gene transcription profiles in mice and humans, we have identified significant alterations in the secretory characteristics of hepatic progenitor cells. The potential impact of these changes in secretory profiles on the hepatic microenvironment remains to be elucidated.

HSCs, although constituting a minority of liver cells, play a crucial role in the pathogenesis and advancement of liver cirrhosis. During homeostasis, they remain

dormant, primarily acting as reservoirs for retinoids or vitamin A-containing metabolites. However, under pathological circumstances, activated and proliferating HSCs transform into myofibroblasts, generating a collagen-rich extracellular matrix (ECM) and inflammatory mediators, thereby exacerbating the progression of liver cirrhosis.^[14] Blocking myofibroblasts is a key target for the treatment of fibrosis.^[15] In this study, we investigated the effects of transplanting HepLPCs into the cirrhosis liver of rats, focusing on their ability to reduce active fibrogenesis and net fibrosis. Additionally, we found that HepLPC-secretomes significantly inhibited TGF- β 1-induced activation of HSCs and induced apoptosis of HSCs in vitro. Notably, primary hepatocyte secretomes did not exhibit a similar effect. Among the soluble factors secreted by HepLPCs, amphiregulin (AREG) and FGF19 were identified as potential mediators of HSC apoptosis, potentially through synergistic activation of signal transducer and activator of transcription (STAT)1 signaling.

METHODS

Animal experiments

All animal procedures were conducted in accordance with the Reporting of In Vivo Experiments guidelines for the care and use of laboratory animals and were approved by the Institutional Animal Care and Use Committee of Shanghai Model Organisms Center Inc. (IACUC2019-0027-06). Animals were kept in an air-filtered, temperature-controlled (22–24°C), light-controlled room with humidity between 40%–70%. All interventions were performed during the light cycle.

Liver cirrhosis model: For the liver cirrhosis model induced by thioacetamide (TAA), male Sprague-Dawley rats aged 5–6 weeks (Vitalriver, China) received TAA (i.p., 200 mg/kg body weight, diluted in saline; Sigma, China) twice a week for 13 weeks.^[16] We maintain TAA drug administration while simultaneously performing cell transplantation, so the total period for rats to receive TAA is 17 weeks.

Liver fibrosis model: 5- to 6-week-old male C57BL/6 mice (Vitalriver, China) were treated with TAA (i.p., 200 mg/kg body weight, diluted in saline; Sigma, China) 3 times a week for 7 weeks.^[17]

Immunosuppressive drug administration: For human HepLPC transplantation, 2 days prior to transplantation, tacrolimus (FK506) was administered to the control group, sham group, and HepLPC group at a dose of 0.2 mg/kg daily until 1 week after cell injection. Rats with rat-HepLPC transplantation did not receive immunosuppressive drugs.

Cell transplantation: the cell transplantation procedure was performed twice. At each cell injection point, 5×10^6 HepLPCs in 500 μ L of PBS were infused into the

rat spleen (day 0). The total number of injected cells into rats with cirrhosis induced by TAA was 1×10^7 per rat. The sham group received an equivalent volume of PBS injection. Rats were sacrificed at 2 weeks after the last cell injection, and samples of liver tissue and blood were collected for further analysis.

Recombinant proteins administration: rhAREG (200 μ g/kg) and rhFGF19 (200 μ g/kg) were administered to mice via the tail vein in a volume of 250 μ L, twice with a 3-day interval. The sham group received an equivalent volume of denatured proteins. Mice were sacrificed at 1 week after TAA administration, and samples of liver tissue and blood were collected for further analysis.

Cell culture

Rat primary hepatocytes were isolated from the livers of Sprague-Dawley rats using a 2-step collagenase perfusion procedure as described elsewhere.^[18] Human primary hepatocytes, purchased from CYTES BIOTECHNOLOGIES, SL., Spain, were cultured following established protocols.^[13]

Passage 5 HepLPCs were used for in vivo experiments. The immortalized human HSC line LX-2 and human primary HSCs were cultured in DMEM supplemented with 2% fetal bovine serum, penicillin (100 U/mL), and streptomycin (100 mg/mL), all obtained from Gibco, USA.

Secretomes preparation

To prepare the secretomes, human HepLPCs were cultured to 60% confluence in culture dishes. After being washed with PBS, the cells were incubated in serum-free DMEM for 24 hours. The conditioned medium was harvested and centrifuged at 300 g to remove cell debris. The supernatant culture medium was collected and concentrated 25-fold using ultrafiltration units with 10-kDa cutoff filters (Amicon Ultra, Millipore).^[17] The secretomes were stored at -80°C until use.

Statistical analyses

Data (mean \pm SD) were analyzed using GraphPad Prism V7. The two-tailed Student *t* test was used to compare the 2 groups. One one-way ANOVA was used for multiple comparisons, followed by Bonferroni test procedure. A two-tailed *p*-value of <0.05 was considered statistically significant.

Additional details regarding materials and procedures, including antibodies (Supplemental Table S1), the biological process in cytokines of LX2 and HepLPCs

co-culture media (Supplemental Table S2), donor information of purchased hepatocytes (Supplemental Table S3), biological networks of enriched proteins in the HepLPC secretomes (Supplemental Table S4), and primers (Supplemental Table S5), are available in the Supplemental Methods and Materials section, accessible via the following link: <http://links.lww.com/HC9/B865>.

RESULTS

Allogeneic HepLPCs attenuated liver fibrosis in rat models of liver cirrhosis

Based on our previous work with mice and established methodologies,^[12] we cultured hepatic progenitor-like cells (HepLPCs) from rats. The rat-derived HepLPCs applied in this study exhibited similar gene expression and growth patterns to those observed in mouse HepLPCs, as reported previously^[12] (Supplemental Figure S1A, B, <http://links.lww.com/HC9/B865>). These rat-derived HepLPCs demonstrated the ability to form spheroids in three-dimensional cultures, exhibiting enhanced hepatic markers and hepatocyte function, as evidenced by immunofluorescence staining, DiI-LDL intake assay, periodic acid-schiff staining, and indocyanine green uptake (Supplemental Figure S1C, D, <http://links.lww.com/HC9/B865>).

Experiments were conducted to investigate whether rat-derived hepatic progenitor-like cells (HepLPCs) could facilitate tissue repair in a rat model of liver cirrhosis. Liver cirrhosis was induced by repeated injections of TAA over 13 weeks and confirmed through hematoxylin and eosin (H&E) staining and picro-Sirius Red staining. Rat-derived HepLPCs, transfected with green fluorescent protein (Supplemental Figure S1E, F, <http://links.lww.com/HC9/B865>), were administered via injection into the spleens of cirrhotic rats (Figure 1A). In this model, we attempted to maintain TAA drug administration while simultaneously performing cell transplantation, hence the cells were transplanted twice. Four weeks later after the initial injection, the sham group still showed fragmented liver nodules and collagen deposition. However, rat-HepLPC injection resulted in a reduction in ECM accumulation and a decrease in the number of activated HSCs, as evidenced by Masson Trichrome, Fibronectin, picro-Sirius Red staining, and α -smooth muscle actin (α -SMA) staining (Figure 1B–D). Moreover, there was a decrease in hydroxyproline levels and a lower fibrosis score in the HepLPCs-treated rats compared to controls (Figure 1E, F), providing further evidence of the amelioration of liver fibrosis. Additionally, favorable effects were observed in serum levels of parameters related to liver function, which decreased following HepLPC transplantation (Figure 1G). Overall, these

findings suggest that HepLPC treatment alleviates liver cirrhosis in TAA-treated rats. Notably, only a few HepLPCs were detectable via green fluorescent protein staining in the liver 2 weeks after the final cell injection (Figure 1H). The possibility of cell delivery to other organs in rat liver cirrhosis models was also explored, revealing no engraftment of rat-derived HepLPCs in other organs, such as the lung, heart, and kidney (Supplemental Figure S1G, <http://links.lww.com/HC9/B865>).

Xenogeneic HepLPCs mimicked the therapeutic effects of allogeneic HepLPCs in the TAA-induced model of cirrhosis

Given the efficacy of rat HepLPCs in treating cirrhosis, along with their short duration of engraftment post-transplantation, we are intrigued by the potential therapeutic effects of human HepLPCs. Previously, we demonstrated the transition and expansion of human hepatocytes in vitro.^[13] Consequently, experiments were conducted to evaluate the feasibility of treating rats with TAA-induced cirrhosis using human HepLPCs. The human HepLPCs employed in this study exhibited gene expression profiles similar to those of rat-HepLPCs (Supplemental Figure S2A–3D, <http://links.lww.com/HC9/B865>). Flow cytometry analysis demonstrated a significant expression (>90%) of HNF4 α , CD24, and CK19, with low expression levels (<2%) of CD34, CD45, and AFP (Supplemental Figure S2E, <http://links.lww.com/HC9/B865>). Furthermore, the human HepLPCs did not express major histocompatibility complex class II antigens histocompatibility antigen-DP, DQ, DR, indicating low immunogenicity, but did express major histocompatibility complex class I antigens histocompatibility antigen-A, B, C, rendering them susceptible to rejection post-transplantation. To counteract this risk, tacrolimus (FK506), an immunosuppressive drug, was administered before transplantation and sustained for 1-week post-injection. No instances of tumorigenesis were observed within 16 weeks following human HepLPC transplantation into NSG mice (Figure S2F, <http://links.lww.com/HC9/B865>).

The establishment of liver cirrhosis and the transplantation of human HepLPCs were conducted following the protocol outlined in Figure 2A. Surprisingly, the therapeutic efficacy of human HepLPCs was also evident in the TAA-induced liver cirrhosis model, manifested by reduced ECM accumulation, amelioration of liver fibrosis, and enhanced liver function (Figure 2B–F). Additionally, we observed heightened proliferation of parenchymal cells and diminished proliferation of nonparenchymal cells in rats treated with HepLPCs (Figure 2G–H). We were impressed by the reparative effects of xenogeneic cells on hepatic fibrotic tissues. Therefore, we investigated the fate of

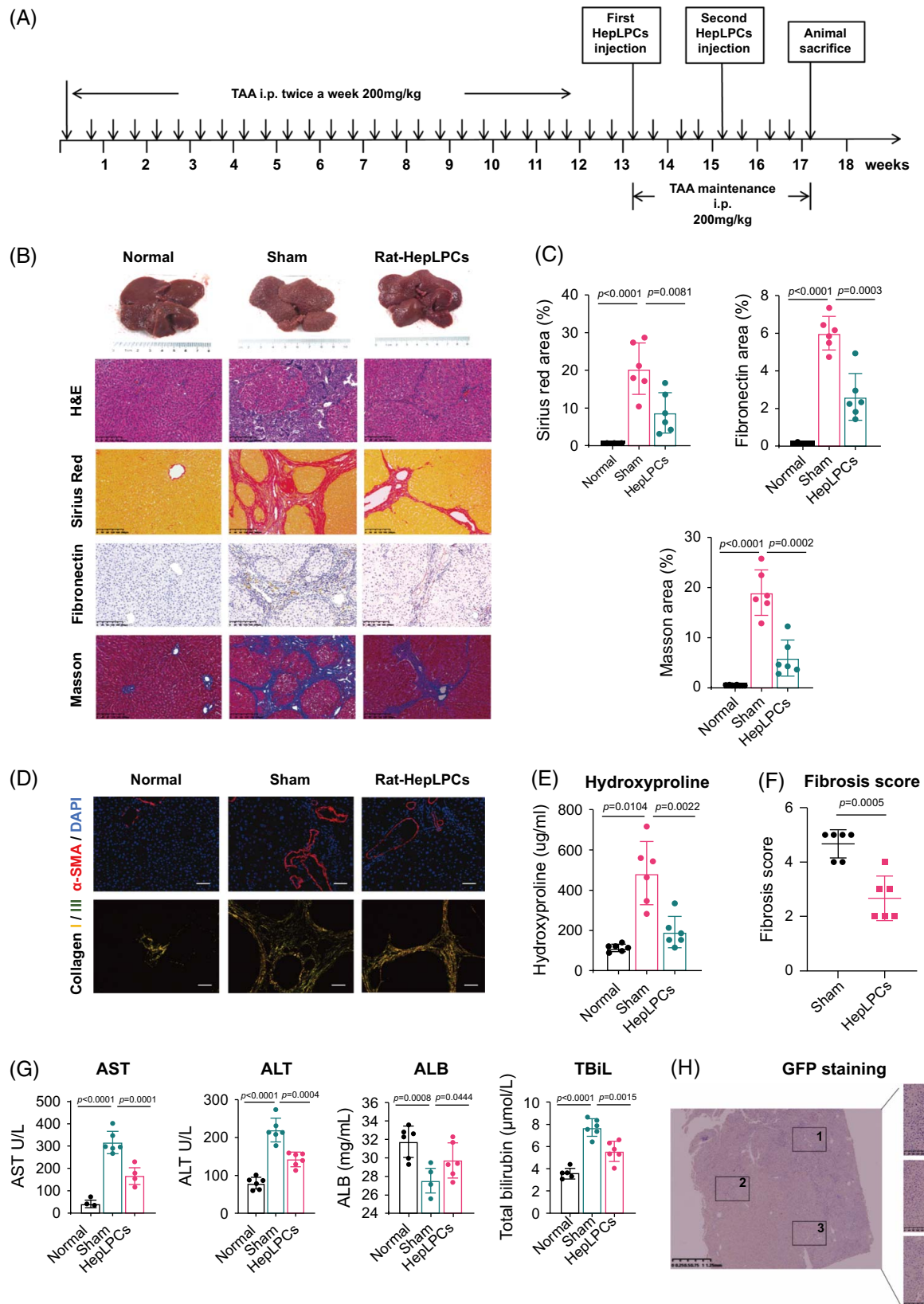


FIGURE 1 The rat-HepLPCs ameliorated rat liver cirrhosis induced by TAA. (A) Schematic overview of the experimental design. (B) Representative images of H&E (hematoxylin and eosin) stained, picro-Sirius Red stained, Fibronectin immuno-stained, and Masson Trichrome stained liver samples, with n=6. Scale bar = 200 μ m. (C) Relative quantification of fibrotic areas and fibronectin-positive stained areas 2 weeks after the last PBS or cell injection. (D) Representative images of α -smooth muscle actin, collagen I, and III in liver samples. Scale bar = 100 μ m. Collagen type I and III quantifications were analyzed under polarized light. With polarizing filters, type I collagen fibers in sections stained with Sirius Red

appear orange to red, and type III collagen fibers appear yellow to green. (E) Quantification of hydroxyproline contents in the liver of cirrhotic rats with indicated treatment. (F) Measurement of liver fibrosis score in cirrhotic rats with indicated treatment. Sections stained with Sirius Red were used for liver fibrosis scoring under the Ishak scoring system. (G) Levels of AST, ALT, ALB (albumin), and TBiL (total bilirubin) in the serum of rats with indicated treatment. (H) Representative images of GFP immunostaining in rat liver with rat-HepLPC treatment. The image on the right is a panoramic view of a liver tissue section, while the images on the left are three randomly magnified local views. Scale bars are depicted in the images. All data are presented as mean \pm SD and analyzed using a two-tailed Student *t* test. The *p*-values are displayed on the bar plot. Abbreviations: ALB, albumin; GFP, green fluorescent protein; H&E, hematoxylin and eosin; HepLPCs, hepatocyte-derived liver progenitor-like cells; TAA, thioacetamide; TBil, total bilirubin.

transplanted cells to elucidate the specific therapeutic mechanisms. Human albumin and HLA-class I antibodies were used to detect human HepLPCs within the rat liver. However, the presence of human HepLPCs in rat livers post-treatment was minimal 2 weeks after the last cell injection (Figure 2I), suggesting that the therapeutic outcomes might be attributed to the secretion of paracrine factors.

HepLPC secretomes exerted an antifibrogenic effect in vitro by inducing HSC apoptosis

In our study on cell therapy for liver cirrhosis in rats, we observed aggregation of nonparenchymal cells within degenerated fibrotic areas in rats with significant remission treated with human HepLPCs. These aggregated cells, which stained positively for α -SMA, exhibited selective induction of apoptosis, as evidenced by heightened signals of cleaved caspase-3 or terminal dUTP nick-end labeling staining in α -SMA-positive cells in representative immunostaining images (Figure 3A). Conversely, no such aggregation was observed in the sham group. In cirrhotic liver tissues, these α -SMA-positive cells also expressed Desmin, indicating their identity as HSCs (Supplemental Figure S3A, <http://links.lww.com/HC9/B865>). These findings suggest that HepLPCs may contribute to the induction of HSC apoptosis.

Based on the findings from in vivo experiments, we hypothesize that HepLPCs may induce apoptosis in HSCs possibly through paracrine secretion. Subsequent experiments were conducted to investigate the antifibrogenic effects of HepLPC-secretomes (HepLPC-scrtns) on HSCs in vitro, using the human HSC cell line LX-2. Real-time polymerase chain reaction experiments demonstrated the inhibition of TGF- β 1-stimulated upregulation of genes related to HSC activation and fibrogenesis by HepLPC-scrtns (Figure 3B). This antifibrogenic effect was confirmed using HepLPC-scrtns derived from 2 other donors (Supplemental Figure S3B, C, <http://links.lww.com/HC9/B865>). Western blot analysis revealed that HepLPC-scrtns decreased the level of fibrosis-related proteins in a dose-dependent manner (Figure 3C). Additionally, HepLPC-scrtns treatment led to reduced

phosphorylation of SMAD2, a critical fibrogenic signaling molecule (Figure 3D). We observed a significant morphological change in LX-2 cells treated with HepLPC-scrtns for an extended period (Figure 3E). Live-cell staining demonstrated reduced viability of LX-2 cells after HepLPC-scrtns treatment (Figure 3F), suggesting that HepLPC-scrtns exerted their antifibrogenic effect by inducing HSC death. PARP and Caspase-3 activation was detected by immunoblotting in LX-2 cells on HepLPC-scrtns administration (Figure 3G). Detection of apoptotic bodies (Figure 3H) and Annexin V/PI flow cytometry (Figure 3I) further confirmed the induction of progressive apoptosis in HSCs by HepLPC-scrtns. Similar results were obtained with human primary HSCs (Supplemental Figure S3D–H, <http://links.lww.com/HC9/B865>). Together, these findings demonstrate that HepLPC secretomes exert an antifibrogenic effect in vitro by inducing apoptosis of HSCs.

HepLPC secretomes induced HSC apoptosis by activating the STAT1 pathway

To identify potential signaling pathways involved in mediating the proapoptotic impact of HepLPC-scrtns on LX-2 cells, we assessed the cytokine expression profiles of the supernatants of LX-2 cells, HepLPCs, and LX-2/HepLPCs co-cultures (Supplemental Figure S4A, <http://links.lww.com/HC9/B865>). The differentially expressed cytokines in the co-culture supernatants were categorized into 10 Gene Ontology terms based on biological processes. Most notably, the majority of these terms were associated with the janus kinase (JAK)-STAT pathway, indicating its positive regulation in LX-2 cells co-cultured with HepLPCs (Figure 4A). Consequently, the phosphorylation and activation statuses of STAT1 and STAT3 in LX-2 cells were evaluated. HepLPC-scrtns treatment resulted in elevated pSTAT1 levels with negligible impact on pSTAT3 (Figure 4B). Pharmacological inhibition of JAK-STAT activation through pre-treatment of LX-2 cells with pyridone 6 significantly attenuated HepLPC-scrtns-induced apoptosis (Figure 4C, D). To validate the specific involvement of STAT1, we silenced STAT1 expression in LX-2 cells using a shRNA targeting human STAT1

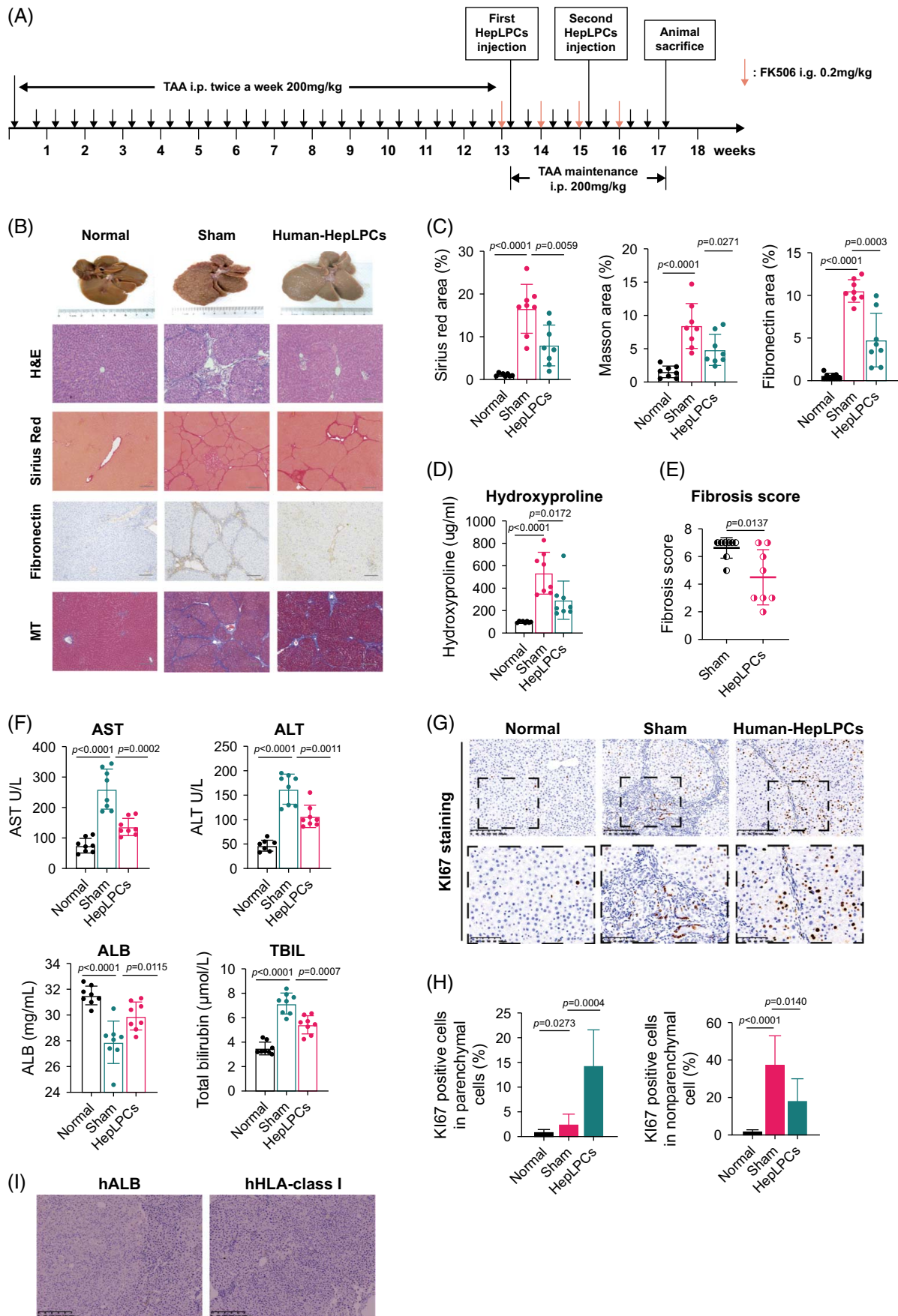


FIGURE 2 Human-HepLPCs attenuated rat liver cirrhosis induced by TAA. (A) A schematic overview of the experimental design. (B) Representative images of H&E stained, picro-Sirius Red stained, Fibronectin immuno-stained, and Masson trichrome stained liver samples, $n = 8$. Scale bar = 200 μm . (C) Relative quantification of fibrotic areas and fibronectin-positive staining areas 2 weeks after the last PBS or cell injection. (D) Quantification of hydroxyproline contents in the liver of cirrhotic rats with indicated treatment. (E) Measurement of liver fibrosis score in cirrhotic rats with indicated treatment. Sections stained with Sirius Red were used for liver fibrosis scoring under the Ishak scoring system. (F) Levels of AST, ALT, ALB, and TBiL in the serum of rats with indicated treatment. Representative images (G) and quantification (H) of Ki67 stained liver samples from rats treated with human HepLPCs or PBS. Scale bars are depicted in the images. (I) Representative images of human ALB, and HLA-class I immunostaining of liver from rats with human HepLPCs therapy for 2 weeks. Scale bar = 300 μm . Throughout, data are mean \pm SD, two-tailed Student *t* test. *p*-values are depicted on the bar plot. Abbreviations: ALB, albumin; H&E, hematoxylin and eosin; HepLPCs, hepatocyte-derived liver progenitor-like cells; HLA, histocompatibility antigen; TAA, thioacetamide; TBil, total bilirubin.

(Supplemental Figure S4B, <http://links.lww.com/HC9/B865>). Both shControl and shSTAT1 LX-2 cells were fluorescently labeled with green fluorescent protein, and Annexin V/7-aminoactinomycin D apoptosis detection kit was employed. As expected, flow cytometric analysis indicated that STAT1 knockdown in LX-2 cells diminished the proapoptotic effect of HepLPC-scrtns, although both shControl and shSTAT1 cells exhibited a slight, nonsignificant increase in necrotic cell count (Figure 4E, F). Re-establishment of STAT1 expression also restored the proapoptotic effect of HepLPC-scrtns treatment (Supplemental Figure S4C–E, <http://links.lww.com/HC9/B865>), affirming that HepLPC-scrtns-induced apoptosis in HSCs was mediated via activation of the STAT1 pathway.

Western blot analysis was conducted to assess the expression of proapoptotic proteins in LX-2 cells, aiming to elucidate downstream targets of STAT1-mediated apoptosis in HSCs induced by HepLPC-scrtns. Treatment with HepLPC-scrtns led to the activation of caspase-8, caspases-3, and caspases-7 cleavage (Figure 4G). In contrast, the expression of apoptosis-modulating proteins was diminished or eradicated in shSTAT1 cells (Figure 4H). Collectively, these findings demonstrate the key role of the STAT1 signaling pathway in mediating HepLPC secretome-induced apoptosis in HSCs.

Identification of antifibrotic agents in the HepLPC secretomes

To further explore the composition of secreted proteins by HepLPCs, we applied tandem mass tags to analyze the proteomic profile of HepLPCs. Control secretomes obtained from primary hepatocytes (PHHs), which had little inhibitory effects on HSC activation *in vitro*, were included for comparison (Supplemental Figure S5A, <http://links.lww.com/HC9/B865>). Four secretomes from HepLPC derived from individuals of diverse genders, races, and ages were compared with PHH-secretomes. A total of 4614 proteins were identified, with 914 proteins exhibiting differential expression between HepLPC-scrtns and PHH-scrtns (Supplemental

Figure S5B, C, <http://links.lww.com/HC9/B865>). Among the identified proteins, 478 were upregulated in HepLPC-scrtns (Figure 5A), indicating distinct protein profiles in HepLPCs compared to PHHs despite their origin from PHHs. Notably, 20.55% of the upregulated proteins were extracellular proteins with known secretory membrane receptors, while 46% were cytoplasmic proteins (Figure 5B). These proteins were quantified based on their mass spectrometry abundance ratios, with 54 proteins exhibiting enrichment of more than 5-fold in HepLPC-scrtns (Figure 5C). Subsequently, these 54 proteins were subjected to analysis using the GeneGo pathway database. The biological networks identified included protein binding, signaling receptor binding, molecular function regulation, identical protein binding, receptor-ligand activity, receptor regulator activity, calcium ion binding, cytokine activity, and growth factor activity (Figure 5D). Protein-protein Interaction (PPI) analysis was used to establish a network linking the JAK-STAT pathway with proteins involved in growth factor activity, cytokine activity, and receptor-ligand activity. The network visualization revealed direct or indirect interactions between leukemia inhibitory factor, endothelin 1, colony-stimulating factor 1 (CSF1), AREG, 19 FGF19, and intermediate molecules of the JAK-STAT pathway (Figure 5E). Western blot analyses of cell-free secretomes confirmed a higher abundance of these five molecules in HepLPC-scrtns compared to PHH-scrtns (Figure 5F).

Validation of FGF19 and AREG as a novel antifibrotic target in liver fibrosis

We used recombinant human (rh) proteins or synthetic peptides of the 5 proteins to assess their agonistic activity on STAT1 signal transduction *in vitro*. Only rhFGF19 (100 ng/mL) and rhAREG (100 ng/mL) showed significant increases in pSTAT1 levels in LX-2 cells in the presence of TGF- β 1 (Figure 6A). Neither protein alone was reported to induce apoptosis in LX-2 cells, prompting further investigation into the synergistic effects of rhFGF19 and rhAREG on STAT1 activation, which may underlie apoptosis in these

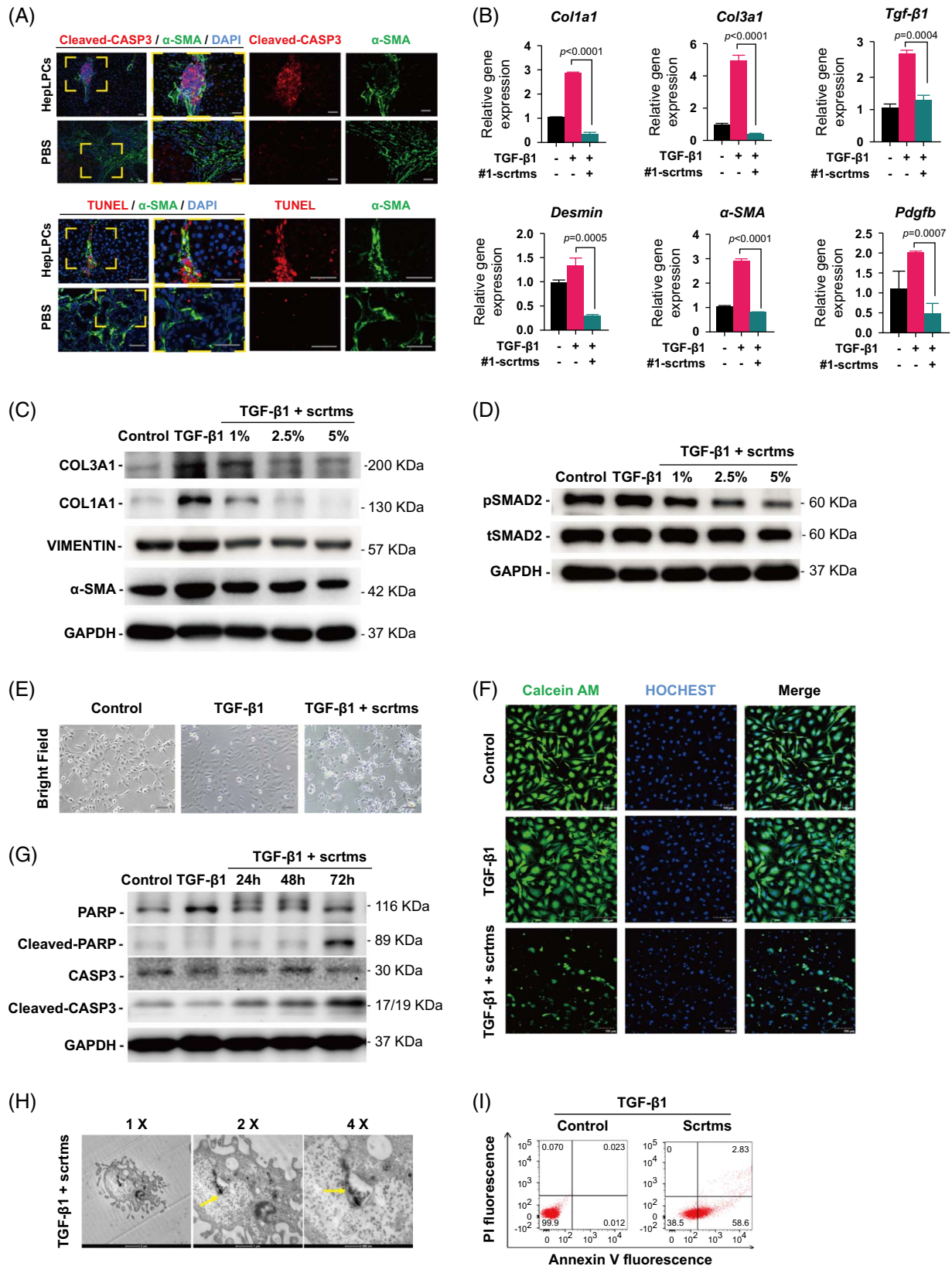


FIGURE 3 HepLPC-secretomes inhibit HSC activation and induce apoptosis in vitro. (A) Representative images of α -SMA and cleaved-CASPASE 3 (cleaved-CASP3) or α -SMA and terminal dUTP nick-end labeling stained liver samples from rats treated with human HepLPCs or PBS. Scale bar = 100 μ m. (B) Relative mRNA expression of genes related to HSC activation in LX-2 cells treated with HepLPC-secretomes derived from donor #1 in the presence of TGF- β 1 for 48 hours. Data were normalized to Gapdh expression (n = 3). (C) Immunoblot analysis of COL3A1, COL1A1, VIMENTIN, and α -SMA in LX-2 cells after treatment with different doses of HepLPC-secretomes in the presence of TGF- β 1 for

48 h. GAPDH served as the internal control. (D) Immunoblot analysis of the SMAD2 pathway in LX-2 cells after treatment with different doses of HepLPC-secretomes in the presence of TGF- β 1 for 48 hours. (E) Morphological changes of LX-2 cells treated with HepLPC-secretomes in the presence of TGF- β 1 for 72 hours. Scale bar = 50 μ m. (F) Live-cell staining of LX-2 cells treated with HepLPC-secretomes in the presence of TGF- β 1 for 72 hours. Scale bar = 100 μ m. Living cells were stained with calcein-AM (green). (G) Immunoblot analysis of PARP, cleaved-PARP, CASP3, cleaved-CASP3 (cleaved-CASPASE3) in LX-2 cells after HepLPC-secretomes treatment. (H) Transmission electron microscope images of apoptotic bodies in LX-2 cells treated with HepLPC-secretomes. Scale bars are as indicated. Yellow arrows indicate apoptotic bodies. (I) Representative flow cytometric plots of Annexin V/PI staining of LX-2 cells after treatment with HepLPC-secretomes in the presence of TGF- β 1 for 72 hours. Abbreviations: CASP3, cysteine-containing aspartic acid specific proteinase 3; HepLPCs, hepatocyte-derived liver progenitor-like cells; PARP, poly(ADP-ribose) polymerase; α -SMA, α -smooth muscle actin.

cells. Increased p-STAT1 levels were observed at a concentration of 10 ng/mL for each protein when both were added together to culture medium (Figure 6B). Western blot analyses of cell-free preparations confirmed higher abundance of these 2 proteins in HepLPC-scrtns compared to PHH-scrtns (Figure 6C). ELISA further validated their secretion levels in HepLPC-scrtns (Figure 6D). Subsequently, neutralizing antibodies targeting either FGF19 or AREG in HepLPC-scrtns inhibited STAT1 signaling activation (Figure 6E, F), suggesting the necessity of synergistic signaling for this process. Additionally, the combination of rhFGF19 and rhAREG induced apoptosis in HSCs, although it did not reach the same level as HepLPC-scrtns alone. Moreover, the addition of neutralizing antibodies against FGF19 and AREG attenuated the proapoptotic effect of HepLPC-scrtns (Figure 6G, H). To further validate the involvement of FGF19 and AREG in the proapoptotic effect of the HepLPC-scrtns, siRNAs were employed to silence AREG and FGF19 in HepLPCs (Supplemental Figure S6A, <http://links.lww.com/HC9/B865>). We observed morphological alterations following the administration of conditional secretomes to LX-2 cells (Supplemental Figure S6B, <http://links.lww.com/HC9/B865>), and evaluated apoptosis induction in HSCs using Annexin V/7-aminoactinomycin D flow cytometry. Although HSC apoptosis induced by HepLPC-secretomes was not completely abolished by the inactivation of FGF19 and AREG, the proapoptotic effect was diminished (Figure 6I, J).

We further verified the therapeutic effects of the 2 factors in TAA-induced liver fibrosis in vivo. After continuous injection of TAA for 7 weeks, the mice were treated with the proteins via tail vein injection twice at a 3-day interval. Histological analyses revealed that rhFGF19 and rhAREG showed antifibrotic effects, regarding both ECM deposition and HSC activation (Figure 7A, B). There was also a lower fibrosis score and a reduction in ALT and AST serum levels in the rhFGF19/rhAREG treated group compared with the control (Figure 7C, D). Together, these experiments provide evidence that the secretion of FGF19 and AREG by HepLPCs forms the fundamental mechanism underlying their antifibrotic properties.

DISCUSSION

There has been a decades-long interest in the application of in vitro expansion of primary hepatocytes for the regenerative treatment of liver diseases.^[19,20] We, along with other research groups, have demonstrated the efficient conversion of hepatocytes into expanding hepatic progenitor cells using defined medium conditions in vitro.^[13,21–23] Our findings showed that both allogeneic and xenogeneic transplantation of HepLPCs attenuated liver fibrosis in rat models of liver cirrhosis.

There has been speculation that 5% of liver cells must be replaced by transplanted cells for therapeutic effects to be observed.^[24] However, despite the evident therapeutic effects, we found a low engraftment efficiency for HepLPCs in treating liver cirrhosis. Consequently, we inferred that the therapeutic outcome might stem from paracrine factors secreted by HepLPCs rather than from the engraftment of exogenous cells. In vitro experiments confirmed that the HepLPC secretomes induced the apoptosis of HSCs, suggesting a potential antifibrotic mechanism. To explore this further, we analyzed cytokine expression profiles of LX-2 cells, HepLPCs, and their co-culture using Gene Ontology analysis, highlighting the involvement of the JAK-STAT pathway. Mounting evidence suggests this pathway's critical role in chronic liver damage and regeneration.^[25–27] STAT proteins, particularly STAT1 and STAT3, play opposing roles in cell growth and survival: STAT1 activation induces growth arrest and apoptosis, whereas STAT3 activation protects against apoptosis.^[28–30] Cross-regulation between STAT1 and STAT3 may underlie the STAT1-dependent pathway of cell death. Treatment with secretomes notably increased pSTAT1 expression in LX-2 cells, while pSTAT3 levels remained largely unaffected. These findings indicate that secretome factors selectively regulate STAT1 activation, suggesting their potential as innovative therapeutic agents.

Proteomic analysis was used to identify and quantify the protein composition of HepLPC secretomes. PHH secretomes, which did not inhibit LX-2 activation in vitro and have been demonstrated to possess a profibrotic effect,^[31] were included as a

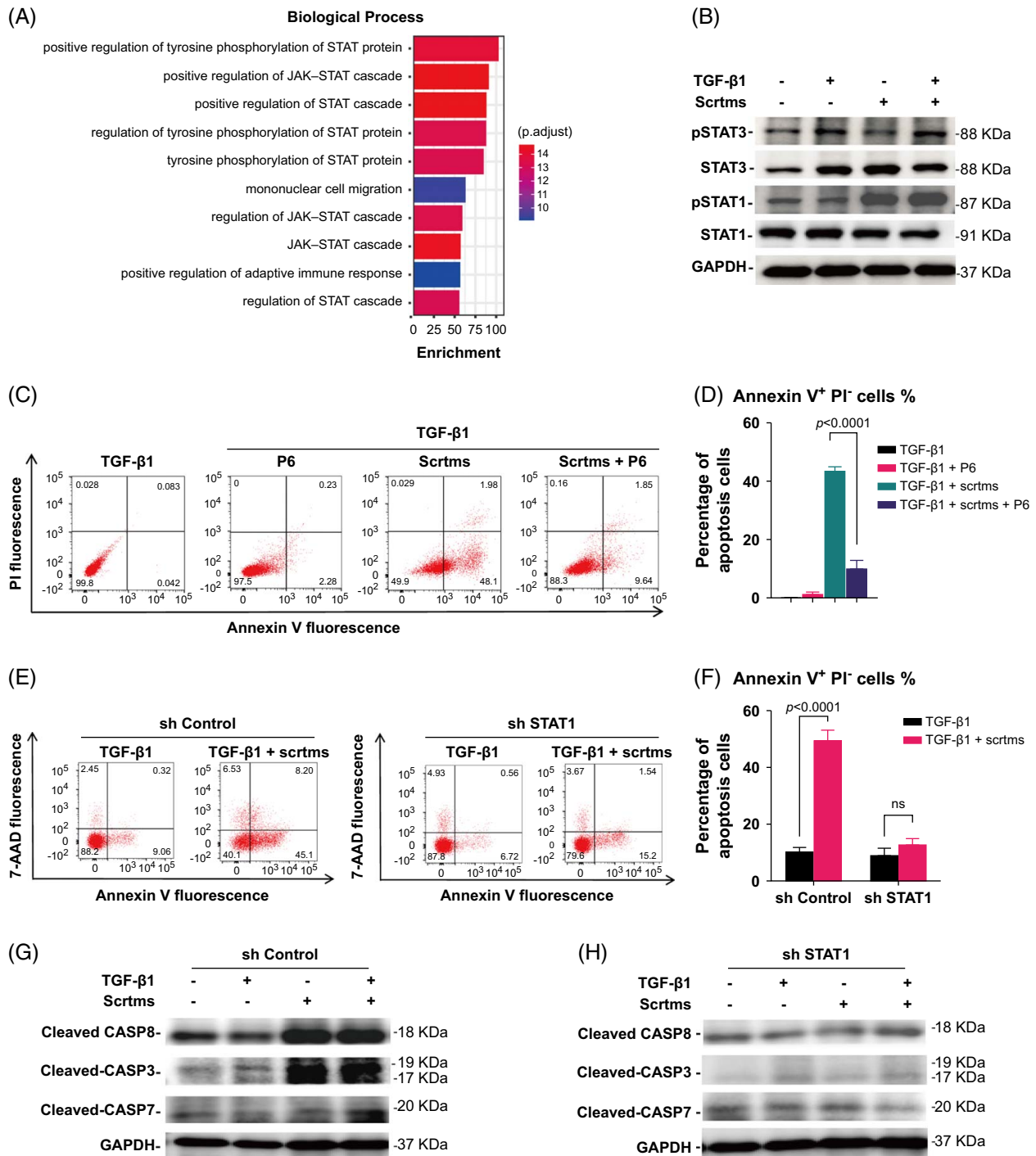


FIGURE 4 STAT1 signaling was required for HepLPC-secretomes-induced apoptosis in HSCs. (A) Gene ontology analysis (biological processes) of differentially expressed cytokines in the co-culture group of culture supernatants. The top 10 GO biological process terms are shown with their associated enrichment values (enrichment = GeneRatio/BgRatio). (B) Immunoblot analysis of STAT3, phospho-STAT3, STAT1, and phospho-STAT1 in LX-2 cells after 72-hour treatment with HepLPC-secretomes. (C, D) Flow cytometry assay (C) and quantification of apoptotic cells (%) (D) in LX-2 cells treated with HepLPC-secretomes in the presence or absence of the JAK activation inhibitor 6 (P6), $n = 3$. (E, F) Flow cytometry assay (E) and quantification of apoptotic cells (%) (F) in LX-2 cells transfected with shControl or shSTAT1 and treated with HepLPC-secretomes, $n = 3$. (G, H) Immunoblot analysis of cleaved-CASPASE8 (cleaved-CASP8), cleaved-CASPASE3 (cleaved-CASP3), and cleaved-CASPASE7 (cleaved-CASP7) in LX-2 cells transfected with shControl (G) or shSTAT1 (H) after 72-hour treatment with HepLPC-secretomes. Throughout, data are presented as mean \pm SD, analyzed using two-tailed Student t test. p -values are indicated on the bar plots. Abbreviations: AAD, aminoactinomycin D; JAK, janus kinase; PI, propidium iodide; STAT, signal transducer and activator of transcription.

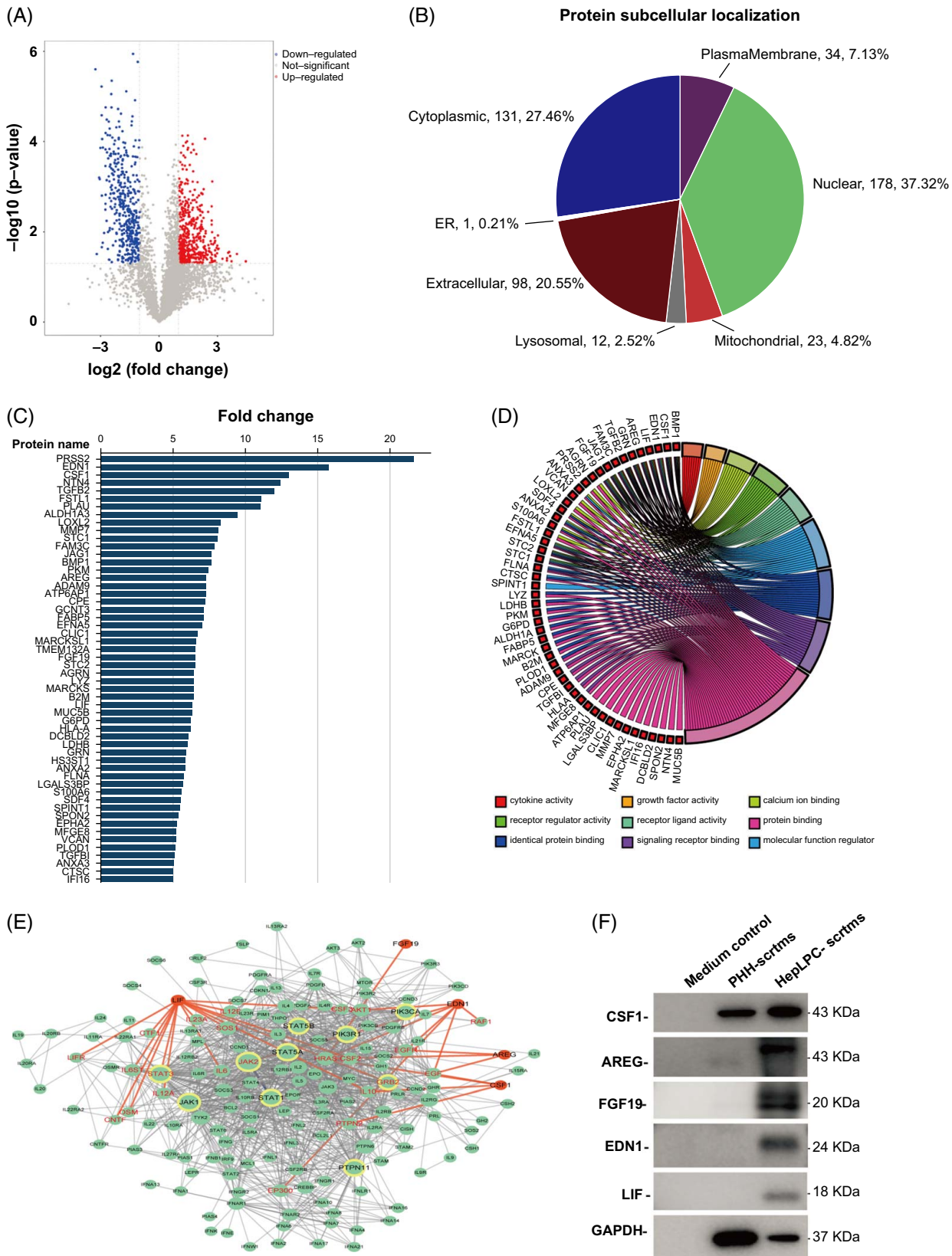


FIGURE 5 Identification of antifibrotic candidates in the secretomes of HepLPCs. (A) Volcano plot analysis of differential protein expression in HepLPC-secretomes (HepLPC-scrtns) compared to PHH-secretomes (PHH-scrtns). Red plots indicate upregulated proteins in HepLPC-scrtns, while blue plots indicate downregulated proteins. (B) Pie chart depicting the subcellular locations of proteins upregulated in HepLPC-scrtns. (C) Analysis of 54 proteins showing > 5-fold higher abundance in HepLPC-scrtns compared to PHH-scrtns. Protein abundance was determined by normalizing the number of identified peptides in tandem mass tag analyses. (D) Gene ontology chart illustrating biological processes associated

with the 54 identified proteins. (E) Potential network interactions of proteins involved in growth factor activity, cytokine activity, and receptor-ligand activity with the JAK-STAT pathway. (F) Immunoblot analysis of cell-free secretomes showing the secretion levels of CSF1, AREG, FGF19, EDN1, and LIF. Abbreviations: AREG, amphiregulin; ER, endoplasmic reticulum; FGF19, fibroblast growth factor 19; HepLPCs, hepatocyte-derived liver progenitor-like cells; LIF, leukemia inhibitory factor; PHHs, primary hepatocytes.

control. To our knowledge, no previous report has systematically documented the proteomic distinctions between hepatic progenitor cells and PHHs. Principal component analysis of HepLPC and PHH secretomes derived from individuals of varying ages, sexes, and races revealed significant similarities in constituent proteomes across donors aged 3 days to 70 years. The proteomic analysis highlighted the presence of growth factors, cytokines, and receptor ligands in HepLPC secretomes, some of which may contribute to STAT1 pathway activation in HSCs. Accordingly, *in vitro* experiments demonstrated that the synergistic effects of FGF19 and AREG could activate STAT1 and induce apoptosis in LX-2 cells, effects attenuated by neutralizing antibodies targeting FGF19 and AREG. Additionally, recombinant FGF19 and AREG exhibited antifibrotic effects in mice with liver fibrosis. Collectively, these findings suggest that FGF19 and AREG may play antifibrogenic roles not only in secretome-mediated antifibrosis but also in the endogenous regulation of hepatic fibrosis.

AREG is expressed in various tissues, including the lung, kidney, and colon. It is barely detectable in a healthy liver but significantly upregulated in a damaged liver, where it appears to have a protective effect.^[32] AREG is a ligand of the tyrosine kinase-linked epidermal growth factor receptor (EGFR), which is a cell surface receptor primarily involved in cell growth. Interestingly, studies have shown that cell lines expressing EGFR can also undergo receptor-mediated apoptosis.^[33,34] However, the mechanism of EGFR-induced apoptosis remains controversial. Studies have shown that signaling molecules such as ERK, STAT, and protein kinase G are involved in this process.^[35–38] The mechanism involves an imbalance caused by increased receptor activity, which can irreversibly disrupt cellular homeostasis and lead to cell death.^[39] Research indicates that activation of EGFR in HSCs by hydrophobic bile salts may result in proliferation or apoptosis, depending on whether other pathways are simultaneously activated. For example, the activation of JNK acts as a switch between EGFR-induced HSC proliferation and apoptosis.^[40] FGF19 is a member of the FGF family involved in the regulation of nutritional metabolism. Analogs of FGF19 have been used to treat metabolic liver diseases, such as NASH and primary sclerosing cholangitis.^[41,42] While FGF19 can reduce Col1 α 1 expression and inhibit HSC proliferation, mechanisms are underexplored.^[43]

Our research found that FGF19 and AREG synergistically induce HSC apoptosis through STAT1 activation, which may provide new insights into receptor-mediated apoptosis mechanisms. In addition, many proteins known to have antifibrotic effects, such as MFGE8,^[44] or hepato-protective effects, such as colony-stimulating factor 1,^[45] were also highly expressed in the HepLPC secretomes. These proteins may contribute to the resolution of liver cirrhosis in animals treated with HepLPCs. However, the current study indicates these proteins have no direct connection with the apoptosis of HSCs.

Here, we have demonstrated the efficacy of HepLPCs in improving liver cirrhosis and provided insights into their underlying mechanisms. Nevertheless, we acknowledge the limitations of our current work. First, we used a single arbitrary cell dosage based on previous experience. Future studies should include dose-response investigations to ascertain both the minimum effective dosage and optimal dosage of cell products. Second, extracellular vesicles, such as exosomes, constitute important components of cell secretomes. Our studies revealed that extracellular vesicles isolated from secretomes minimally impacted the apoptosis of HSCs (data not shown). FGF19 and AREG have been identified as key functional antifibrotic factors in secretomes, necessitating further research to elucidate their roles in liver cirrhosis development. Additionally, due to the complex composition of HepLPC-secretomes, more investigations are warranted to explore their effects on various cell types beyond HSCs. Finally, considering pharmacodynamic factors are crucial in defining clinical application protocols, further research is needed to explore the distribution of cells in different organs over time *in vivo*.

In summary, the paracrine actions of HepLPCs make them a promising therapeutic cell source for the treatment of liver cirrhosis. Identifying therapeutic molecules and elucidating paracrine factors and their mechanisms of action are crucial prerequisites for developing safe and effective cell-based or cell-free derivative therapies. In our study, we have identified the antifibrotic effect of HepLPC secretomes. Specifically, components such as FGF19 and AREG are shown to primarily induce this effect by promoting apoptosis of HSCs through STAT1 activation. Therefore, the future application of HepLPCs or their secretomes to other liver diseases appears highly promising.

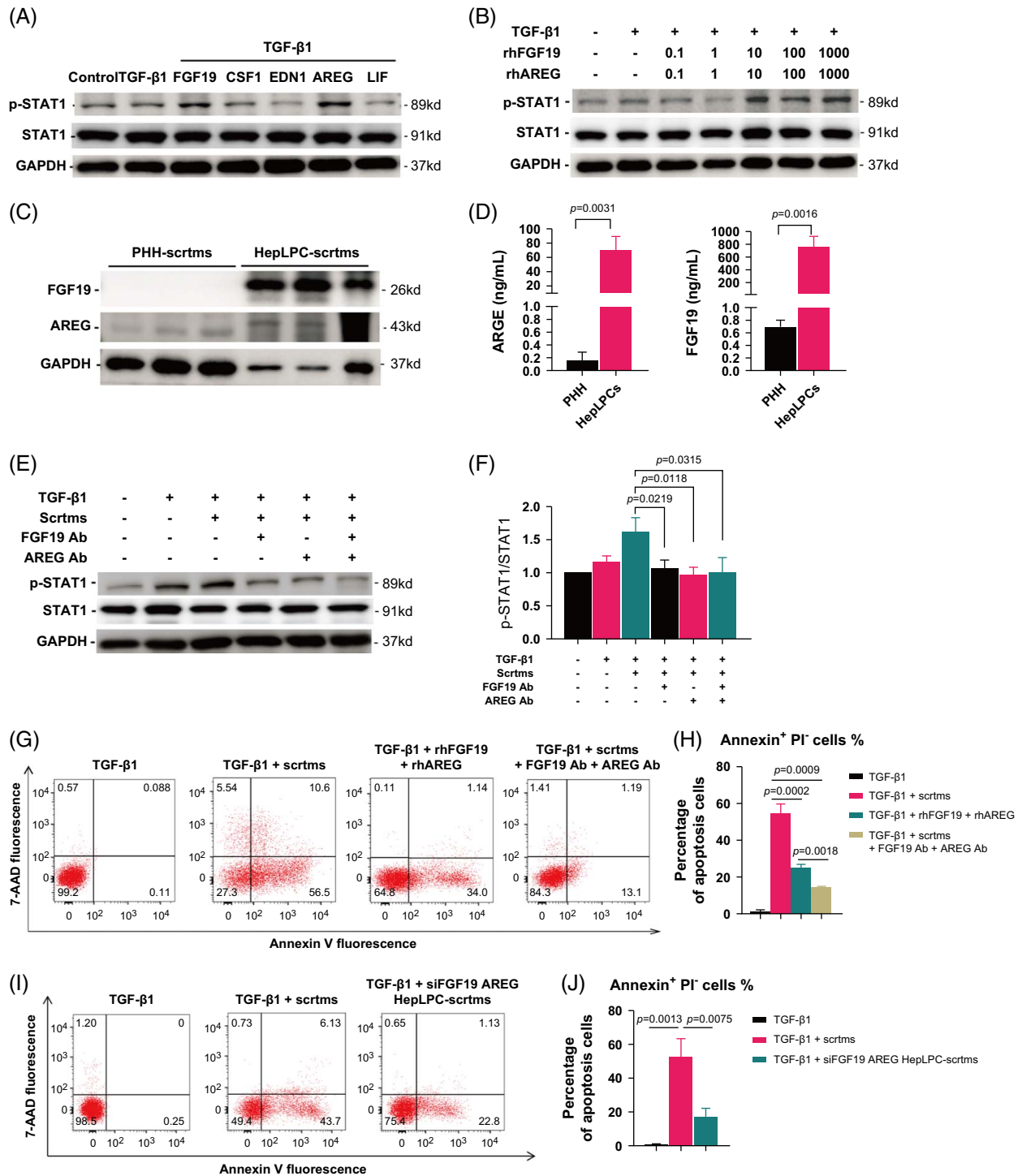


FIGURE 6 FGF19 and AREG in secretomes synergistically induced HSC apoptosis by activating STAT1 pathway. (A) Western blot analysis of STAT1 and phospho-STAT1 in LX-2 treated with indicated human recombinant proteins or synthetic peptides for 72 hours. (B) Dose titration analysis of the combination of rhFGF19 and rhAREG on activation of STAT1 signal in LX-2. LX-2 cells were treated with different doses of rhAREG and rhFGF19 as indicated for 72 hours in the presence of TGF- β 1. (C) Western blot images depicting AREG and FGF19 protein expression in secretomes derived from HepLPCs and PHHs from three independent individuals. (D) ELISA validation of AREG and FGF19 secretion levels from HepLPC and PHH secretomes (n = 3). (E) Western blot images showing phospho-STAT1 levels in LX-2 cells treated with the indicated treatments. (F) Quantification of phospho-STAT1 expression normalized to total STAT1 levels (n = 3). (G) Representative cytometric plots illustrating apoptotic cells in LX-2 cells treated with indicated secretomes. (H) Quantification of apoptotic cells (%) in LX-2 cells treated with indicated secretomes (n = 3). (I) Representative cytometric plots illustrating apoptotic cells in LX-2 cells treated with indicated secretomes. (J) Quantification of apoptotic cells (%) in LX-2 cells treated with secretomes derived from HepLPCs transfected with siFGF19 and siAREG compared to control (n = 3). Throughout, data are mean \pm SD, two-tailed Student *t* test. *p*-values are depicted on the bar plot. Abbreviations: AAD, aminoactinomycin D; AREG, amphiregulin; CSF1, colony-stimulating factor 1; EDN1, endothelin 1; FGF19, fibroblast growth factor 19; LIF, leukemia inhibitory factor; PHHs, primary hepatocytes; PI, propidium iodide; STAT, signal transducer and activator of transcription.

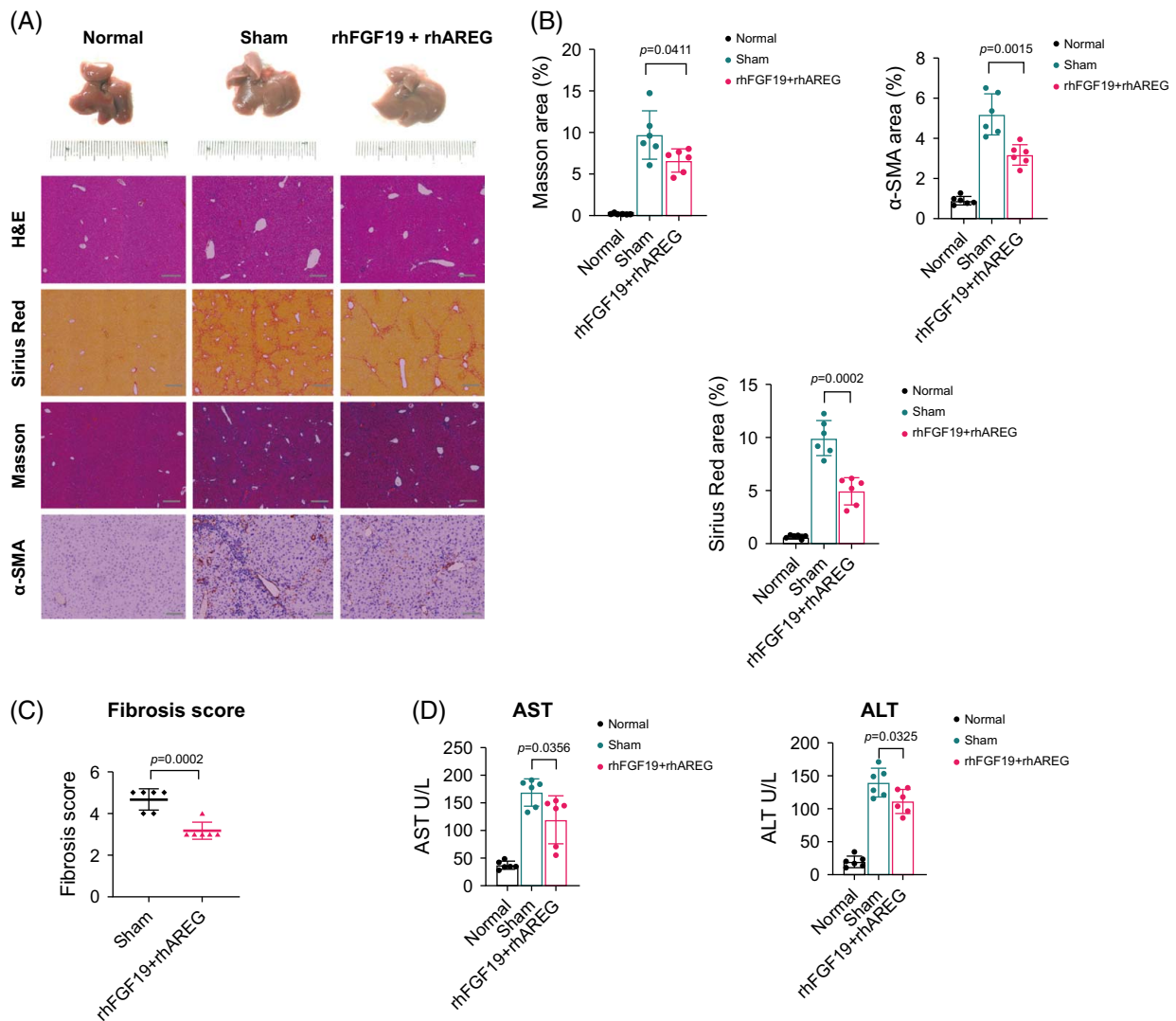


FIGURE 7 FGF19 and AREG as a novel antifibrotic target in liver fibrosis. (A) Representative images of H&E stained, picro-Sirius Red stained, Masson Trichrome stained, and α -SMA stained liver samples from control mice or mice administrated with rhFGF19/rhAREG, $n=6$. Scale bar = 100 μ m. (B) Quantification of fibrotic areas in fibrotic mice after 1 week of treatment with indicated recombinant proteins. (C) Measurement of liver fibrosis scores in fibrosis mice after 1 week with indicated treatment. (D) Levels of AST and ALT in the serum of mice with indicated treatment. Abbreviations: AREG, amphiregulin; FGF19, fibroblast growth factor 19; H&E, hematoxylin and eosin; α -SMA, α -smooth muscle actin.

DATA AVAILABILITY STATEMENT

Data, analytic methods, and study material will be made available to other researchers upon request from the corresponding author.

AUTHOR CONTRIBUTIONS

CRediT Authorship Contributions: Xu Zhou, PhD (conceptualization: lead; data curation: lead; formal analysis: lead; methodology: lead; project administration: lead; writing-original draft: lead). Wen-Ming Liu, MS (data curation: supporting; formal analysis: supporting; methodology: supporting). Han-Yong Sun, PhD (data curation: supporting; formal analysis: supporting; methodology: supporting). Yuan Peng, MD (formal analysis: supporting; methodology: supporting). Ren-Jie Huang,

BS (methodology: supporting; project administration: supporting). Cai-Yang Chen, PhD (funding acquisition: supporting). Hong-Dan Zhang, MS (project administration: supporting). ShenAo Zhou, PhD (methodology: supporting). Hong-Ping Wu, BS (data curation: supporting). Dan Tang, MD (methodology: supporting). Wei-Jian Huang, PhD (methodology: supporting). Han Wu, PhD (funding acquisition: supporting). Qi-Gen Li, PhD (methodology: supporting). Bo Zhai, PhD (supervision: lead; funding acquisition: supporting). Qiang Xia, PhD (supervision: lead; writing-review and editing: lead). Wei-Feng Yu, PhD (supervision: lead; writing-review and editing: lead; funding acquisition: supporting). He-Xin Yan, PhD (conceptualization: lead; funding acquisition: lead; supervision: lead; writing-review and editing: lead).

ACKNOWLEDGMENTS

The authors thank all study participants for efforts and time. The authors thank Sai-Hong Xu and Yi Chen for expert care of animals. The authors also thank Yu-Ling Wu, Xiao-Shu Qi, and Hong-Qian Ma for the assistance with animal experiments.

FUNDING INFORMATION

This work was supported by the National Natural Science Foundation of China (82300700, 81800563, 82070619, 82100671, 82272999), the National Key R&D Program of China (2024YFA1107601), Shanghai Engineering Research Center of Perioperative Organ Support and Function Preservation (20DZ2254200), Clinical Research Plan of SHDC (NO. SHDC2020CR4036), and Shanghai Celliver Biotechnology Co. Ltd.

CONFLICTS OF INTEREST

Ren-Jie Huang, Hong-Dan Zhang, and Shen-Ao Zhou are full-time employees of Shanghai Celliver Biotechnology Co. Ltd. Shanghai, China. H-X.Y. and B.Z. are co-founders of Shanghai Celliver Biotechnology Co. Ltd., Shanghai, China and have an equity interest in Celliver Biotechnology Inc. The remaining authors have no conflicts to report.

REFERENCES

- Devarbhavi H, Asrani SK, Arab JP, Narthey YA, Pose E, Kamath PS. Global burden of liver disease: 2023 update. *J Hepatol.* 2023;79:516–37.
- Gines P, Krag A, Abraldes JG, Sola E, Fabrellas N, Kamath PS. Liver cirrhosis. *Lancet.* 2021;398:1359–76.
- Asrani SK, Devarbhavi H, Eaton J, Kamath PS. Burden of liver diseases in the world. *J Hepatol.* 2019;70:151–71.
- Liu P, Mao Y, Xie Y, Wei J, Yao J. Stem cells for treatment of liver fibrosis/cirrhosis: Clinical progress and therapeutic potential. *Stem Cell Res Ther.* 2022;13:356.
- Forbes SJ, Gupta S, Dhawan A. Cell therapy for liver disease: From liver transplantation to cell factory. *J Hepatol.* 2015;62(1 Suppl):S157–69.
- Fitzpatrick E, Mitry RR, Dhawan A. Human hepatocyte transplantation: State of the art. *J Intern Med.* 2009;266:339–57.
- Schmelzer E, Zhang L, Bruce A, Wauthier E, Ludlow J, Yao HL, et al. Human hepatic stem cells from fetal and postnatal donors. *J Exp Med.* 2007;204:1973–87.
- Cardinale V, Wang Y, Carpino G, Cui CB, Gatto M, Rossi M, et al. Multipotent stem/progenitor cells in human biliary tree give rise to hepatocytes, cholangiocytes, and pancreatic islets. *Hepatology.* 2011;54:2159–72.
- Lanzoni G, Oikawa T, Wang Y, Cui CB, Carpino G, Cardinale V, et al. Concise review: clinical programs of stem cell therapies for liver and pancreas. *Stem Cells.* 2013;31:2047–60.
- Giancotti A, D'Ambrosio V, Como S, Pajno C, Carpino G, Amato G, et al. Current protocols and clinical efficacy of human fetal liver cell therapy in patients with liver disease: A literature review. *Cytotherapy.* 2022;24:376–84.
- Wang J, Li Q, Li W, Mendez-Sanchez N, Liu X, Qi X. Stem cell therapy for liver diseases: Current. Perspectives *Front Biosci (Landmark Ed).* 2023;28:359.
- Wu H, Zhou X, Fu GB, He ZY, Wu HP, You P, et al. Reversible transition between hepatocytes and liver progenitors for in vitro hepatocyte expansion. *Cell Res.* 2017;27:709–12.
- Fu GB, Huang WJ, Zeng M, Zhou X, Wu HP, Liu CC, et al. Expansion and differentiation of human hepatocyte-derived liver progenitor-like cells and their use for the study of hepatotropic pathogens. *Cell Res.* 2019;29:8–22.
- Kisseleva T, Brenner D. Molecular and cellular mechanisms of liver fibrosis and its regression. *Nat Rev Gastroenterol Hepatol.* 2021;18:151–66.
- Caligiuri A, Gentilini A, Pastore M, Gitto S, Marra F. Cellular and molecular mechanisms underlying liver fibrosis regression. *Cells.* 2021;10:2759.
- Yovchev MI, Xue Y, Shafritz DA, Locker J, Oertel M. Repopulation of the fibrotic/cirrhotic rat liver by transplanted hepatic stem/progenitor cells and mature hepatocytes. *Hepatology.* 2014;59:284–95.
- An SY, Jang YJ, Lim HJ, Han J, Lee J, Lee G, et al. Milk fat globule-EGF factor 8, secreted by mesenchymal stem cells, protects against liver fibrosis in mice. *Gastroenterology.* 2017;152:1174–86.
- Shen L, Hillebrand A, Wang DQH, Liu M. Isolation and primary culture of rat hepatic cells. *J Vis Exp.* 2012;64:3917.
- Haridass D, Narain N, Ott M. Hepatocyte transplantation: Waiting for stem cells. *Curr Opin Organ Transplant.* 2008;13:627–32.
- Kwak KA, Cho HJ, Yang JY, Park YS. Current perspectives regarding stem cell-based therapy for liver cirrhosis. *Can J Gastroenterol Hepatol.* 2018;2018:4197857.
- Zhang K, Zhang L, Liu W, Ma X, Cen J, Sun Z, et al. In vitro expansion of primary human hepatocytes with efficient liver repopulation capacity. *Cell Stem Cell.* 2018;23:806–819. e804.
- Peng WC, Logan CY, Fish M, Anbarchian T, Aguisanda F, Álvarez-Varela A, et al. Inflammatory cytokine TNF α promotes the long-term expansion of primary hepatocytes in 3D culture. *Cell.* 2018;175:1607–619 e1615.
- Hu H, Gehart H, Artegiani B, López-Iglesias C, Dekkers F, Basak O, et al. Long-term expansion of functional mouse and human hepatocytes as 3D organoids. *Cell.* 2018;175:1591–1606. e1519.
- Dhawan A, Puppi J, Hughes RD, Mitry RR. Human hepatocyte transplantation: Current experience and future challenges. *Nat Rev Gastroenterol Hepatol.* 2010;7:288–98.
- Park O, Wang H, Weng H, Feigenbaum L, Li H, Yin S, et al. In vivo consequences of liver-specific interleukin-22 expression in mice: Implications for human liver disease progression. *Hepatology.* 2011;54:252–61.
- Jeong WI, Park O, Radaeva S, Gao B. STAT1 inhibits liver fibrosis in mice by inhibiting stellate cell proliferation and stimulating NK cell cytotoxicity. *Hepatology.* 2006;44:1441–51.
- Zhang H, Chen F, Fan X, Lin C, Hao Y, Wei H, et al. Quantitative proteomic analysis on Activated Hepatic Stellate Cells reversion reveal STAT1 as a key regulator between Liver Fibrosis and recovery. *Sci Rep.* 2017;7:44910.
- Zhao J, Qi YF, Yu YR. STAT3: A key regulator in liver fibrosis. *Ann Hepatol.* 2020;21:100224.
- Tang LY, Heller M, Meng Z, Yu LR, Tang Y, Zhou M, et al. Transforming growth factor-beta (TGF-beta) directly activates the JAK1-STAT3 axis to induce hepatic fibrosis in coordination with the SMAD pathway. *J Biol Chem.* 2017;292:4302–12.
- Hong F, Jaruga B, Kim WH, Radaeva S, El-Assal ON, Tian Z, et al. Opposing roles of STAT1 and STAT3 in T cell-mediated hepatitis: Regulation by SOCS. *J Clin Investig.* 2002;110:1503–13.
- An P, Wei LL, Zhao S, Sverdlov DY, Vaid KA, Miyamoto M, et al. Hepatocyte mitochondria-derived danger signals directly activate hepatic stellate cells and drive progression of liver fibrosis. *Nat Commun.* 2020;11:2362.

32. Wu Q, Chen J, Hu X, Zhu Y, Xie S, Wu C, et al. Amphiregulin alleviated concanavalin A-induced acute liver injury via IL-22. *Immunopharmacol Immunotoxicol.* 2020;42:473–83.
33. Sun T, Wu D, Deng Y, Zhang D. EGFR mediated the renal cell apoptosis in rhabdomyolysis-induced model via upregulation of autophagy. *Life Sci.* 2022;309:121050.
34. Hognason T, Chatterjee S, Vartanian T, Ratan RR, Ernewein KM, Habib AA. Epidermal growth factor receptor induced apoptosis: Potentiation by inhibition of Ras signaling. *FEBS Lett.* 2001;491:9–15.
35. Ali R, Brown W, Purdy SC, Davisson VJ, Wendt MK. Biased signaling downstream of epidermal growth factor receptor regulates proliferative versus apoptotic response to ligand. *Cell Death Dis.* 2018;9:976.
36. Sooro MA, Zhang N, Zhang P. Targeting EGFR-mediated autophagy as a potential strategy for cancer therapy. *Int J Cancer.* 2018;143:2116–25.
37. Jackson NM, Ceresa BP. EGFR-mediated apoptosis via STAT3. *Exp Cell Res.* 2017;356:93–103.
38. Jackson NM, Ceresa BP. Protein Kinase G facilitates EGFR-mediated cell death in MDA-MB-468 cells. *Exp Cell Res.* 2016;346:224–32.
39. Reinehr R, Haussinger D. CD95 death receptor and epidermal growth factor receptor (EGFR) in liver cell apoptosis and regeneration. *Arch Biochem Biophys.* 2012;518:2–7.
40. Sommerfeld A, Reinehr R, Haussinger D. Bile acid-induced epidermal growth factor receptor activation in quiescent rat hepatic stellate cells can trigger both proliferation and apoptosis. *J Biol Chem.* 2009;284:22173–83.
41. Rinella ME, Lieu HD, Kowdley KV, Goodman ZD, Alkhouri N, Lawitz E, et al. A randomized, double-blind, placebo-controlled trial of aldafermin in patients with NASH and compensated cirrhosis. *Hepatology.* 2024;79:674–89.
42. Hirschfield GM, Chazouillères O, Drenth JP, Thorburn D, Harrison SA, Landis CS, et al. Effect of NGM282, an FGF19 analogue, in primary sclerosing cholangitis: A multicenter, randomized, double-blind, placebo-controlled phase II trial. *J Hepatol.* 2019;70:483–93.
43. Wang Y, Gunewardena S, Li F, Matye DJ, Chen C, Chao X, et al. An FGF15/19-TFEB regulatory loop controls hepatic cholesterol and bile acid homeostasis. *Nat Commun.* 2020;11:3612.
44. Jang YJ, An SY, Kim JH. Identification of MFGE8 in mesenchymal stem cell secretome as an anti-fibrotic factor in liver fibrosis. *BMB Rep.* 2017;50:58–9.
45. Stutchfield BM, Antoine DJ, Mackinnon AC, Gow DJ, Bain CC, Hawley CA, et al. CSF1 restores innate immunity after liver injury in mice and serum levels indicate outcomes of patients with acute liver failure. *Gastroenterology.* 2015;149:1896–1909. e1814.

How to cite this article: Zhou X, Liu W, Sun H, Peng Y, Huang R, Chen C, et al. Hepatocyte-derived liver progenitor-like cells attenuate liver cirrhosis via induction of apoptosis in hepatic stellate cells. *Hepatol Commun.* 2025;9:e0614. <https://doi.org/10.1097/HC9.0000000000000614>